



Hydrogen Production From catalytic reforming of greenhouse gases (CO₂ and CH₄) Over Neodymium (III) oxide supported Cobalt catalyst

*¹Bamidele, V. Ayodele; ²Uchechukwu Herbert Offor; ¹Osariemen, Edokpayi; ¹Christopher, E. Akhabue; ¹Ejiroghene, T. Akhiero; ³Chin Kui Cheng

^aDepartment of Chemical Engineering, University of Benin, Benin Cit, Nigeria
^bDepartment of Chemical and Petroleum Engineering, University of Uyo, Uyo, Nigeria
^cFaculty of Chemical & Natural Resources Engineering, Universiti Malaysia Pahang, Lebuhraya Tun Razak, 26300 Gambang Kuantan, Pahang Malaysia
*Corresponding author E-mail: ¹bamidele.ayodele@uniben.edu

ABSTRACT: Hydrogen production from CO₂ reforming of methane over 20wt%.Co/Nd₂O₃ has been investigated in a fixed bed stainless steel reactor. The 20wt%.Co/Nd₂O₃ catalyst was synthesized using wet impregnation method and characterized for thermal stability, textural property, crystallinity, morphology and nature of chemical bonds using techniques such as TGA, XRD, N₂ adsorption-desorption, FESEM, EDX and FTIR. The CO₂ reforming of methane was performed at feed ratio (CH₄:CO₂) between 0.1-1 and reaction temperature ranged 973-1023 K. The catalyst displayed good activity towards selectivity and yield of hydrogen as well as CO, a by product. The selectivity and yield of Hydrogen increases with feed ratio and reaction temperature. The 20wt%.Co/Nd₂O₃ catalyst displayed promising catalytic activity for hydrogen production with the highest yield and selectivity of 32.5% and 17.6% respectively.

© JASEM

<https://dx.doi.org/10.4314/jasem.v21i6.9>

Keywords: Cobalt; Greenhouse gases; Hydrogen; Reforming;; Neodymium (III)Oxide

Since the first synthetic production of Hydrogen in the early 16th century, there has been a lot of technological advancement in the production process through research and development (National Hydrogen Association, 2010). Nowadays, hydrogen can be produced using varieties of feedstocks mostly from fossil and renewable resources (Balat & Kirtay, 2010; Kirtay, 2011). Hydrogen production from fossil resources include coal or biomass gasification and natural gas reforming using steam, O₂ or CO₂ (Salkuyeh & Adams, 2013).

The production of hydrogen from coal gasification became popular during the oil crisis in the late 1970s (Self, Reddy, & Rosen, 2012). During gasification, coal is broken down into H₂, syngas and CO₂ (Li, Zhang, & Bi, 2010). Coal gasification presently account for 15% commercial global hydrogen production (Man et al., 2014). However, the process is major contributory to the emissions of greenhouse gases (Man et al., 2014). Hydrogen production using steam reforming is a well developed and mature technology. Presently, about 48% of the world commercial production of hydrogen is produced from steam reforming (IEA, 2006). The production of hydrogen by steam methane reforming involve two primary reactions namely reforming and water gas shift reaction represented in Equations (1) and (2) respectively (Koo et al., 2014).



Although, steam methane reforming is a well established process for hydrogen production, challenges of catalyst deactivation has been a major

concerns of researches over the years (Sehested, 2006). Nickel catalysts which is commonly used for the steam methane reforming process is easily susceptible to catalyst deactivation from poisoning, sintering and carbon depositions (Legras, et al., 2014). Besides catalyst deactivation, CO₂ produced from steam methane reforming process is one of the key components of greenhouse gases responsible for global warming.

A more environmental friendly process for hydrogen production is by utilizing both CO₂ and CH₄, key principal components of greenhouse gases as feedstock for hydrogen or syngas production (Equation (3)) (Braga et al., 2014). Besides, the advantage of mitigating greenhouse gases emissions, CO₂ reforming of methane is also suitable for production of H₂/CO ratio < 2 suitable as chemical intermediate for the production of synthetic fuel via Fischer-Tropsch synthesis (Yao et al., 2011). The CO₂ reforming of methane is however not fully developed into commercial process due to constraint from catalyst deactivation mainly from carbon deposition (Ruckenstein & Wang, 2002).



Literature review by Budiman et al. (2012) shows that several metal-based catalysts such as Pt, Ir, Co, Pd, Ru, Rh and Ni have been investigated for CO₂ reforming of methane as reported. Amongst these metal catalysts, Rh and Ru have been shown to have the highest activities and good thermal stability. However, these catalysts are not economical for large scale production. Ni-based catalysts which are

inexpensive have been widely studied and reported to have good catalytic activity (Gonçalves, et al., 2006; Ryi et al., 2013). Nevertheless, these catalysts are easily prone to catalytic deactivation from sintering and carbon deposition (Sehested, 2006)

Supported Co catalysts have been reported to have comparable catalytic activity and stability to Ni-catalysts (Budiman et al., 2013). Studies have also shown that supported Co catalysts are stable at high temperature during CO₂ reforming of methane (Luisetto et al., 2012). Co-based catalysts has been synthesis by impregnating aqueous solution of the Co precursors into supports such as CeO₂, ZrO₂, MgO, Al₂O₃, SiO₂, TiO₂ (Budiman et al., 2012; Budiman et al., 2013). These supports have been reported to have effects on the catalytical behavior and the extent of carbon depositions on the catalysts.

Significantly, rare earth metal oxides such as CeO₂, ZrO₂ and La₂O₃ have been shown to have good features as catalyst supports due to their high oxygen retention capacity (Abasaheed et al., 2015; Fonseca et al., 2014). High catalytic activity and stability was reported for CeO₂ and ZrO₂ supported Co catalysts for hydrogen production from CO₂ reforming of methane (Abasaheed et al. 2015). Sokolov et al. (2012) reported that the addition of La₂O₃ to ZrO₂ supported Ni catalysts significantly increased the catalytic activity and stability. The catalyst was shown to have no distortion in activity over 180 h time-on-stream. Literature on the use of Nd₂O₃ supported Co catalyst for Hydrogen production from CO₂ reforming of methane is very scarce.

In the present study, catalytic performance of Nd₂O₃ supported Co catalyst for hydrogen production via CO₂ dry reforming is investigated. The Nd₂O₃ support was prepared by thermal decomposition of Neodymium (III) nitrate hexahydrate at 773 K for 2 h and subsequently used for synthesis of the Co catalyst by wet impregnation method.

MATERIALS AND METHOD

Catalysts preparation: The schematic diagram of the catalyst preparation is depicted in Figure 1. First, the catalyst support (Nd₂O₃) was synthesized by thermal decomposition of Nd(NO₃)₃.6H₂O (99.99% purity, Sigma-Aldrich) at 773 K for 2 h (Mohammadinasab et al., 2014). The 20wt.% Co/Nd₂O₃ catalyst was prepared by wet impregnation method. Aqueous solution of Co(NO₃)₂.6H₂O (99.99% purity, Sigma-Aldrich) equivalent to 20wt.% Co loading was impregnated into the Nd₂O₃ support. The mixture was continuously stirred for 3 h, followed by drying at 393 K for 24 h and calcination at 873 K for 5 h.

Catalyst characterization: The as-synthesized 20wt.%Co/Nd₂O₃ catalyst was characterized for physicochemical properties by temperature

programmed calcination, N₂ adsorption-desorption isotherm, X-ray diffraction, Fourier transform infrared spectroscopy (FTIR), field emission scanning electroscopy (FESEM), energy dispersion X-ray spectroscopy (EDX) and particle size distribution analysis. Information about the thermal stability of the fresh 20wt.%Co/Nd₂O₃ catalyst was obtained from temperature programmed calcination using thermal gravimetric analyzer (TA instruments, Q500). The catalyst sample was calcined under the flow of compressed air (99.99% purity) from room temperature to 1173 K. The thermal stability of the catalysts was analyzed as a function of weight loss (%) and the derivative weight loss (%/K) using Platinum software. The analysis for the BET specific surface area and pore volume was done by liquid N₂ adsorption-desorption at 77 K using Thermo scientific surfer analyzer. The BET surfer instrument consist of two components namely the analyzer and the sample preparation degasser. The catalyst sample was degassed at 573 K in a vacuum for 3 h. The pore volume and pore diameters were estimated from the desorption section of the N₂ adsorption-desorption isotherm using modeled derived by Barrett, Joyner and Halenda (BJH) (Huang et al., 2014). The crystallinity of the catalyst was obtained from XRD diffractograms which were collected on a RIGAKU miniflex 600 diffractograms using Cu K α ($\lambda=0.154$ nm) radiation. The nature of chemical bonds of the catalyst was determined by Thermo Scientific FT-IR (Nicolet iS 50) spectrometer. The sample spectra was collected within wave number 4000-500 cm⁻¹ using attenuated total reflectance. Morphology and elemental composition of the catalyst were determined by FESEM equipped with EDX. The particle size distribution was done by mastersizer particle size analyzer (Mastersizer 2000). **Catalytic activity:** The catalytic activity of the 20wt.% Co/Nd₂O₃ catalyst for H₂ production via CO₂ reforming of methane was performed in a fixed bed stainless steel reactor. The catalyst weighing 200 mg was supported with quartz wool in the fixed bed reactor which was vertically positioned in a furnace with four heating zones. The temperature of the catalytic bed was monitored by a Type-K thermocouple. Prior to the commencement of the reforming reaction, the catalyst was reduced *in situ* under flow of 60 ml/min of H₂/N₂ (1:5). The CO₂ reforming of methane over the 20wt.% Co/Nd₂O₃ was performed at reaction temperature ranging from 973 to 1123 K at 1 bar and gas hourly speed velocity of 30000 mmol/gcatalyst/min. The feed ratio of the reactant (CH₄:CO₂) was varied between 0.1 and 1 to determine its effect on yield and selectivity. The composition of the products (H₂ and CO) as well as the reactants were analyzed by a gas chromatography (GC) equipped with thermal conductivity conductor (TCD) (Agilent, Q 6400). The product yield and selectivity were calculated using Equation (4) –(7) respectively.

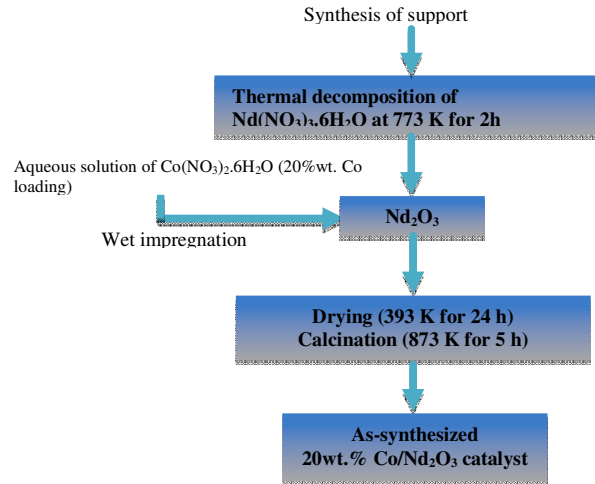


Fig 1: Schematic diagram for 20wt.% Co/Nd₂O₃ catalyst preparation

$$H_2 \text{ yield (\%)} = \frac{F_{H_2, \text{out}}}{2F_{CH_4, \text{in}}} \quad (4)$$

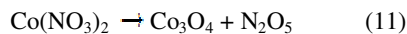
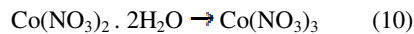
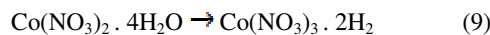
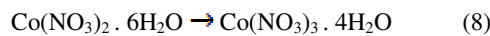
$$CO \text{ yield (\%)} = \frac{F_{CO, \text{out}}}{2(F_{CH_4, \text{in}} + F_{CO_2, \text{in}})} \quad (5)$$

$$H_2 \text{ selectivity (\%)} = \frac{F_{H_2, \text{out}}}{F_{H_2, \text{out}} + F_{CH_4, \text{in}} + F_{CO_2, \text{in}} + F_{CO}} \quad (6)$$

$$CO \text{ selectivity (\%)} = \frac{F_{CO}}{F_{CH_4, \text{in}} + F_{CO_2, \text{in}} + F_{CO}} \quad (7)$$

RESULT AND DISCUSSIONS

Catalyst characterization: The thermal stability analysis by temperature programmed calcination of the fresh catalyst is depicted in Figure 2. Significantly, four stages (I-IV) of weight losses can be identified from the temperature programmed calcination (Equation (8) –(11)).



Stage I-III (Equation (1) – (3)) could be attributed to sequential loss in both physical and hydrated water (Foo et al., 2011). Decomposition of Co(NO₃)₂ to obtained Co₃O₄ could be assigned to stage four.

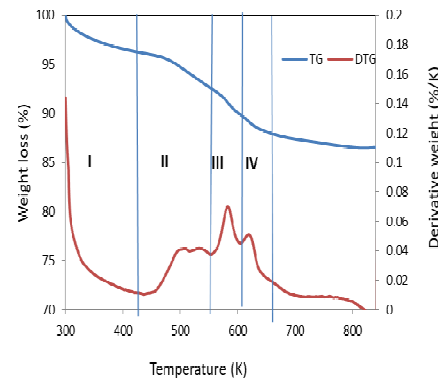


Fig 2: Temperature programmed calcination of the fresh 20wt.%Co/Nd₂O₃ catalyst.

Figure 3 shows type IV N₂ adsorption-desorption isotherm of the 20wt.%Co/Nd₂O₃ catalyst. This signifies that the catalyst is mesoporous with pore volume of 0.0061 cm³ and average pore diameter of 2.19 nm. The catalyst exhibited BET surface areas of 18.67 m²/g.

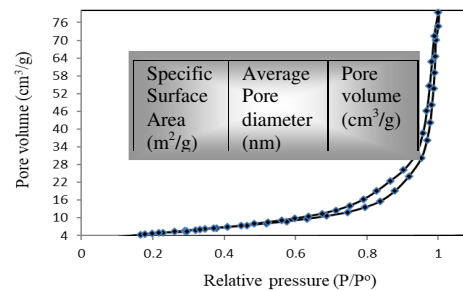


Fig 3: N₂ physisorption isotherm of the fresh 20wt.%Co/Nd₂O₃ catalyst.

The XRD pattern of the fresh 20wt.%Co/Nd₂O₃ catalyst is depicted in Figure 4. The XRD diffraction peaks $2\theta = 16.17, 23.80, 38.71, 40.64, 41.59, 44.80, 50.02$ and 70.59° correspond to spinel Co₃O₄ while those $2\theta = 27.08, 31.05, 33.74, 48.40$ and 60.21 can be attributed to Nd₂O₃.

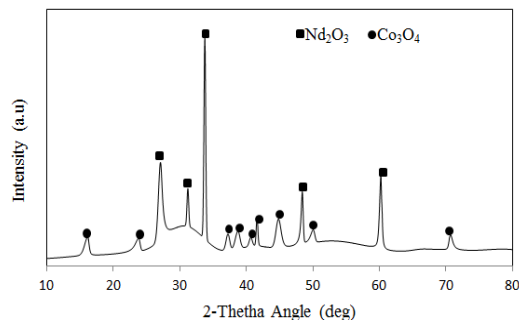


Fig 4: XRD pattern of the fresh 20wt.%Co/Nd₂O₃ catalyst.

Information on the nature of metallic bond that exists in the as-synthesized 20wt.%Co/Nd₂O₃ is depicted in Figure 4. The FTIR spectra display band at 3417, 1489, 790 and 634 cm⁻¹ respectively. The band at 3417 and 1489 cm⁻¹ can be attributed to atmospheric moisture and dissolved CO₂ respectively. Band 790 and 634 cm⁻¹ can be attributed to medium vibration metal-oxide (M-O) bonds due to the presence of Co-O and Nd-O respectively (Kępiński et al., 2004).

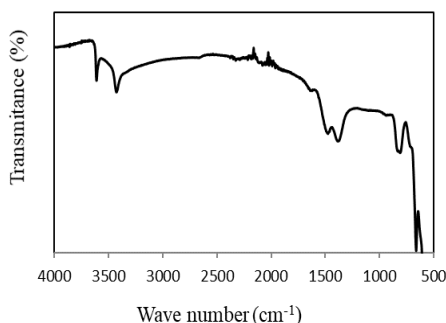


Fig 5: FTIR spectra of the fresh 20wt.%Co/Nd₂O₃ catalyst

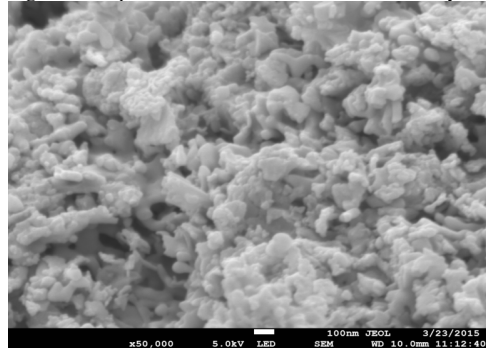


Fig 6: FESEM image of the fresh 20wt.%Co/Nd₂O₃ catalyst

The morphology and elemental composition of the as-synthesized 20wt.%Co/Nd₂O₃ catalyst represented the FESEM image and EDX micrograph are depicted in Figure 5 and 6 respectively. The agglomeration of catalyst particles can be seen from the FESEM image while the elemental compositions of the as-synthesized 20wt.%Co/Nd₂O₃ catalyst is consistent with that obtained from the EDX micrograph (Figure 5). This further confirms the efficiency of employing wet impregnation method for catalyst preparation.

The catalytic performance of the 20wt.%Co/Nd₂O₃ in terms of yield of H₂ and CO as well as syngas (H₂+CO) at feed ratio and temperature ranged 0.1-1 and 923 – 1023 K respectively; are depicted in Figures 10–12. It is noteworthy that H₂, CO and the syngas yield increases with feed ratios for all the reaction temperatures. However, the catalyst shows better activity towards H₂ production as it is evident from the highest yield of H₂ produced compared to CO (Naem et al., 2014). Similar trend by Ibrahim et al. (2014) was also observed in their study on hydrogen production via CO₂ reforming of methane over strontium promoted Alumina supported Ni and Co catalysts. This implies that CO₂ reforming of methane over 20wt.%Co/Nd₂O₃ is a potential technological route for the production of H₂.

The particle size distribution of the 20wt.%Co/Nd₂O₃ catalyst on volume-based is depicted in Figure 7. The d₁₀, d₅₀ and d₉₀ of the catalyst particles are 3.991 μm, 22.44 μm and 70.96 μm respectively. The particle distributions of the catalyst is within the stipulated range that will not influence to the effect of mass transfer on the rate of reaction (Gribb & Banfield, 1997).

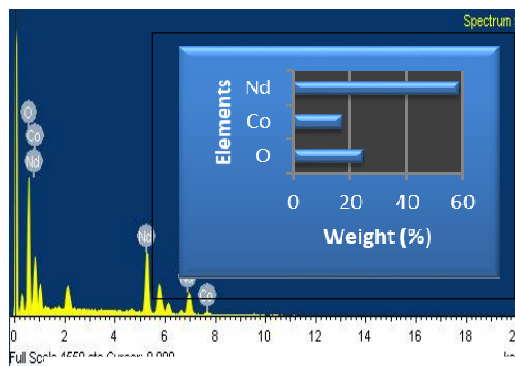


Fig 7: EDX Monograph showing the elemental composition of the fresh 20wt.%Co/Nd₂O₃ catalyst

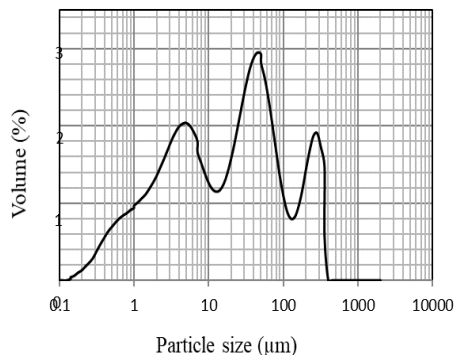


Fig 8: Particle size distribution of the fresh 20wt%.Co/Nd₂O₃ catalyst

Effect of feed ratio and temperature on product selectivity and yield: The CO₂ reforming of methane was performed over 20wt%.Co/Nd₂O₃ catalyst. The catalytic performance of the 20wt%.Co/Nd₂O₃ catalyst as function of H₂ and CO yields in the CO₂ reforming of methane are depicted in Figures 8 and 9 respectively. Significantly, the selectivity of both H₂ and CO increases with feed ratio and temperature with the highest values obtained at feed ratio and temperature of 1 and 1023 K respectively. However, the catalyst shows a higher selectivity towards H₂ production than CO. This trend is consistent with the findings of Tu & Whitehead (2014) and Naeem et al. (2014). The findings from both studies shows that H₂ selectivity increases as the temperature increase from 773 to 1073 K..

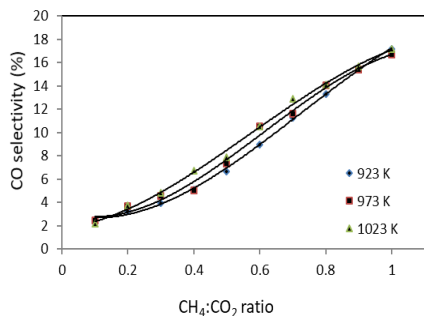


Fig 9: Effect of feed ratio and temperature the on 20wt%.Co/Nd₂O₃ catalyst selectivity toward H₂

Conclusion: In this study, the production of H₂ and CO via CO₂ reforming of methane over 20wt%.Co/Nd₂O₃ catalyst has been investigated. The CO₂ reforming of methane reaction was performed at temperature ranged 923-1023K and feed ratios between 0.1 and 1.. The best catalytic activities of the 20wt%.Co/Nd₂O₃ catalyst in terms of yield and selectivity were recorded at 1023 K and feed ratio of 1. The catalyst characterization corroborate the catalytic performance of the 20wt%.Co/Nd₂O₃ catalyst in terms of yield and selectivity of the products of the methane dry reforming

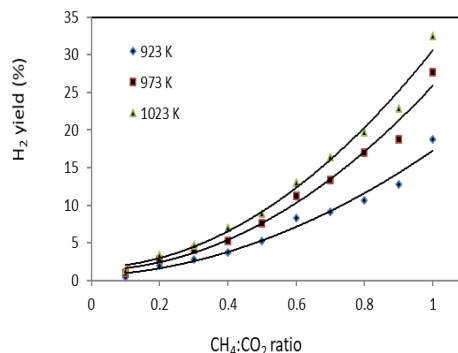


Fig 10: Effect of feed ratio and temperature the on 20wt% Co/Nd₂O₃ catalyst selectivity toward CO

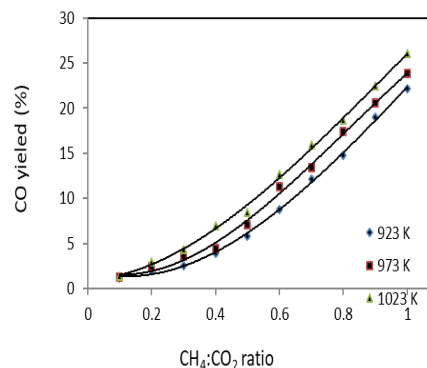


Fig 11: Effect of feed ratio and temperature the on 20wt%.Co/Nd₂O₃ catalyst activity toward H₂ yield

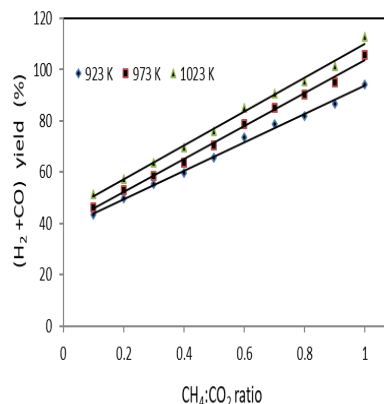


Fig 12: Effect of feed ratio and temperature the on 20wt% .Co/Nd₂O₃ catalyst activity toward syngas (H₂ + CO) yield

REFERENCES

- Abasaheed, AE; Al-fatesh, AS; Naeem, MA; Ibrahim, AA; Fakeeha, AH (2015). Catalytic performance of CeO₂ and ZrO₂ supported Co catalysts for hydrogen production via dry reforming of methane. *International of Hydrogen Energy*, (40), 6818–6826.

- Balat, H; Kirtay, E. (2010). Hydrogen from biomass - Present scenario and future prospects. *International Journal of Hydrogen Energy*, 35(14), 7416–7426.
- Braga, TP; Santos, RCR; Sales, BMC; da Silva, BR; Pinheiro, AN; Leite, ER; Valentini, A (2014). CO₂ mitigation by carbon nanotube formation during dry reforming of methane analyzed by factorial design combined with response surface methodology. *Chinese Journal of Catalysis*, 35(4), 514–523.
- Budiman, A; Ridwan, M; Kim, SM; Choi, JW; Yoon, CW; Ha, JM; Suh, YW (2013). Design and preparation of high-surface-area Cu/ZnO/Al₂O₃ catalysts using a modified co-precipitation method for the water-gas shift reaction. *Applied Catalysis A: General*, 462-463, 220–226.
- Budiman, AW; Song, SH; Chang, TS; Shin, CH; Choi, MJ (2012). Dry Reforming of Methane Over Cobalt Catalysts: A Literature Review of Catalyst Development. *Catalysis Surveys from Asia*, 16(4), 183–197.
- Fonseca, ROD; Da Silva, AA; Signorelli, MR; Rabelo-Neto, RC; Noronha, FB; Simões, RC; Mattos, LV (2014). Nickel / Doped Ceria Solid Oxide Fuel Cell Anodes for Dry Reforming of Methane. *Journal of the Brazilian Chemical Society*, 25(12), 2356–2363.
- Foo, SY; Cheng, CK; Nguyen, TH; Adesina, AA (2011). Kinetic study of methane CO₂ reforming on Co–Ni/Al₂O₃ and Ce–Co–Ni/Al₂O₃ catalysts. *Catalysis Today*, 164(1), 221–226.
- Gonçalves, G; Lenzi, MK; Santos, OAA; Jorge, LMM (2006). Preparation and characterization of nickel based catalysts on silica, alumina and titania obtained by sol–gel method. *Journal of Non-Crystalline Solids*, 352(32-35), 3697–3704.
- Gribb, AA; Banfield, JF (1997). Particle size effects on transformation kinetics and phase stability in nanocrystalline TiO₂. *Journal of the Mineralogical Society of America*, 82(7-8), 717–728.
- Huang, B; Bartholomew, CH; Woodfield, BF (2014). Improved calculations of pore size distribution for relatively large, irregular slit-shaped mesopore structure. *Microporous and Mesoporous Materials*, 184, 112–121.
- Ibrahim, AA; Fakeeha, AH; Al-Fatesh, AS (2014). Enhancing hydrogen production by dry reforming process with strontium promoter. *International Journal of Hydrogen Energy*, 39(4), 1680–1687.
- IEA. (2006). Hydrogen Production and Storage. *International Energy Agency*, 13, 392–392.
- Kępiński, L; Zawadzki, M; Miśta, W (2004). Hydrothermal synthesis of precursors of neodymium oxide nanoparticles. *Solid State Sciences*, 6(12), 1327–1336.
- Kirtay, E (2011). Recent advances in production of hydrogen from biomass. *Energy Conversion and Management*, 52(4), 1778–1789.
- Koo, KY; Lee, S; Jung, UH; Roh, HS; Yoon, WL (2014). Syngas production via combined steam and carbon dioxide reforming of methane over Ni–Ce/MgAl₂O₄ catalysts with enhanced coke resistance. *Fuel Processing Technology*, 119, 151–157.
- Legras, B; Ordonsky, VV; Dujardin, C; Virginie, M; Khodakov, AY (2014). Impact and Detailed Action of Sulfur in Syngas on Methane Synthesis on Ni/γ-Al₂O₃ Catalyst, (111).
- Li, K; Zhang, R; Bi, J (2010). Experimental study on syngas production by co-gasification of coal and biomass in a fluidized bed. *International Journal of Hydrogen Energy*, 35(7), 2722–2726.
- Luisetto, I; Tuti, S; Di Bartolomeo, E (2012). Co and Ni supported on CeO₂ as selective bimetallic catalyst for dry reforming of methane. *International Journal of Hydrogen Energy*, 37, 15992–15999.
- Man, Y; Yang, S; Xiang, D; Li, X; Qian, Y (2014). Environmental impact and techno-economic analysis of the coal gasification process with/without CO₂ capture. *Journal of Cleaner Production*, 71, 59–66.
- Mohammadinasab, R; Tabatabaee, M; Aghaie, H; Seyed Sadjadi, MA (2014). A Simple Method for Synthesis of Nanocrystalline Sm₂O₃ Powder by Thermal Decomposition of Samarium Nitrate. *Synthesis and Reactivity in Inorganic, Metal-Organic, and Nano-Metal Chemistry*, 45(3), 451–454.
- Naeem, MA; Al-Fatesh, AS; Fakeeha, AH; Abasaheed, AE (2014). Hydrogen production from methane dry reforming over nickel-based nanocatalysts using surfactant-assisted or polyol method. *International Journal of Hydrogen Energy*, 39(30), 17009–17023.
- National Hydrogen Association. (2010). History of Hydrogen Timeline. *New York State Energy Research and Development Authority*, 1–2.
- Ruckenstein, E; Wang, HY (2002). Carbon Deposition and Catalytic Deactivation during CO₂ Reforming of CH₄ over Co/γ-Al₂O₃ Catalysts. *Journal of Catalysis*, 205(2), 289–293.
- Ryi, S; Lee, S; Park, J; Oh, D; Park, J; Kim, S (2013). Combined steam and CO₂ reforming of methane using catalytic nickel membrane for gas to liquid (GTL) process. *Catalysis Today*, 236, 49–56.
- Salkuyeh, YK; Adams, TA (2013). Combining coal gasification, natural gas reforming, and external carbonless heat for efficient production of gasoline and diesel with CO₂ capture and sequestration. *Energy Conversion and Management*, 74, 492–504.
- Sehested, J (2006). Four challenges for nickel steam-reforming catalysts. *Catalysis Today*, 111(1-2), 103–110.
- Self, SJ; Reddy, BV; Rosen, MA (2012). Review of underground coal gasification technologies and carbon capture. *International Journal of Energy and Environmental Engineering*, 3(1), 16.